NUCLEAR THEORY, Vol. 35 (2016)
eds. M. Gaidarov, N. Minkov, Heron Press, Sofia

Systematic Effects in the Measurement of the Negatively Charged Pion Mass Using Laser Spectroscopy of Pionic Helium Atoms

B. Obreshkov

Institute for Nuclear Research and Nuclear Energy
Bulgarian Academy of Sciences, Sofia 1784, Bulgaria

Abstract.

The collision-induced shift and broadening of selected dipole transition lines of pionic helium in gaseous helium at low temperatures up to $T = 12$ K and pressure up to a few bar are calculated within variable phase function approach. We predict blue shift of the resonance frequencies of the $(n, l) = (16, 15) \rightarrow (16, 14)$ and $(16, 15) \rightarrow (17, 14)$ unfavored transitions and red shift for the favored transition $(17, 16) \rightarrow (16, 15)$. The result may be helpful in reducing the systematic error in proposed future experiments for determination of the negatively charged pion mass from laser spectroscopy of metastable pionic helium atoms.

1 Introduction

Pionic atom spectroscopy permits to measure the charged pion mass. Orbital energies of the system depend on the reduced mass of the system. These energies can be calculated with high precision using quantum electrodynamics (QED). Measuring transition frequencies, not disturbed by strong interactions, allows to determine the reduced mass of the system and hence the mass of the pion.

Two experiments at Paul Scherrer Institute (PSI) using X-ray spectroscopy of pionic atoms gave most precise values for the masses of the muon-type neutrino and of the charged pion. By measuring the energy of the X-ray emitted in the 4f-3d transition of pionic magnesium, the pion mass was measured to 3 parts per million (ppm) accuracy [1, 2]. However the experiment found a negative value for the square of the muon neutrino mass. Re-analysis of the Mg-atom data including better model of electron screening corrections, lead to a pion mass compatible with positive mass squared of the muon-type neutrino.

Because of the complexity of the electronic structure of pionic magnesium, more recently a method for laser spectroscopy of pionic helium atoms has been proposed [3]. Pionic helium is a three-body system composed of a helium nucleus, an electron in a ground state and π^- in highly excited nearly circular state with principal and orbital quantum numbers $n \sim l+1$. These states can de-excite

via Auger transitions to lower lying states which have large overlap with the helium nucleus and subsequently undergo fast nuclear absorption for times less than a picosecond. However long-lived π^- were observed in bubble-chamber experiments [4], to explain this anomaly, Condo [5] suggested that metastable atomic states of π^- are formed

$$\mathrm{He} + \pi^- \rightarrow [\mathrm{He}^+\pi^-]_{nl} + e^- \,, \tag{1}$$

in which π^- occupies highly excited Rydberg states with principal quantum number $n \sim (m^*/m_e)^{1/2} \sim 16$, where m^* is the reduced mass of π^- and the helium nucleus. For nearly circular orbits $n \sim l + 1$, the Auger decay rate is strongly suppressed and because the radiative decay $\tau_{\mathrm{rad}} \sim 1\ \mu s$ is also slow, the lifetime of the metastable states is determined by the proper lifetime of π^-, $\tau_{\pi^-} \sim 26$ ns. An indirect conformation of the Condo's hypothesis has been obtained at TRIUMF [6] in experiments with π^- stopped in liquid helium; it has been found that about 2% of the pions retain a lifetime of 7 ns.

When comparing experimental transition frequencies to three-body QED calculations of pionic helium, the π^- mass can be determined with fractional precision better than 1 ppm [7]. However systematic effects such as collision-induced shift and broadening of the transition lines, the collision quenching of the metastable pionic states, AC Stark shifts, frequency chirp in the laser beam, can prevent the experiment from achieving this high precision. Reliable theoretical calculation for the density-dependent shift and width is needed for the extrapolation of transition wavelengths at zero target density.

2 Line Shift and Broadening Calculations

2.1 Interatomic potentials

The collisional shift and broadening of the laser stimulated transition line in pionic helium are obtained in the impact approximation of the binary collision theory of the spectral line shape [8–11]. The interaction energy between the pionic and ordinary helium atoms is obtained in the Born-Oppenheimer approximation by separating adiabatically the electronic from the nuclear degrees of freedom. The potential energy surface (PES) for the description of the binary interaction between an exotic helium with ordinary helium atom had been evaluated with ab initio quantum chemistry methods [12, 13] for nearly 400 configurations of the two helium nuclei and the pion. The nuclear configurations are parameterized with the length r of the vector joining the heavy particles in the pionic atom, the length R of the vector joining its center-of-mass with the nucleus of the perturbing helium atom, and the angle θ between them. Subsequently, the numerical values of the PES at these 400 grid points were fitted with smooth functions $V(r, R, \theta)$ and used in the calculation of the collisional shift and dephasing rate. Because the collisional quenching due to inelastic collisions at thermal energies is unlikely to be relevant for the metastable states of the pionic atom, we use

central state-dependent potentials to describe the elastic scattering

$$V_{nl}(R) = \frac{1}{2}\int dr|\chi_{nl}(r)|^2 \int d\theta \sin\theta V(r,R,\theta), \tag{2}$$

where $\chi_{nl}(r)$ are the unperturbed π^- wave-functions.

2.2 Impact approximation

When the helium gas atoms are moving rapidly, the broadening and shift the spectral lines arises from a series of binary encounters between the pionic atom with ordinary helium atom. The impact approximation is valid if the average time interval between collisions is much larger than the duration of the collision [9]. For an isolated spectral line produced by a laser-stimulated dipole transition from an initial state $i = (n, l)$ to a final state $f = (n', l')$ of the pionic atom, the line shape assumes a Lorentizan profile

$$I_{fi}(\omega) = \frac{|\mathbf{d}_{fi}|^2}{\pi}\frac{\Gamma_{fi}}{(\omega - \omega_{fi} + \Delta_{fi})^2 + \Gamma_{fi}^2}, \tag{3}$$

where $\mathbf{d}_{fi}$ is the transition dipole moment, $\omega_{fi} = E_f - E_i$ is the transition frequency and Γ_{fi} and Δ_{fi} are the collision-induced broadening and shift, respectively. In the approximation of binary collisions, both the shift $\Delta_{fi} = N\beta_{fi}$ and the polarization dephasing rate $\Gamma_{fi} = N\alpha_{fi}$ are linear functions of the gas density N. The slope of the temperature-dependent collisional broadening and shift are

$$\alpha_{fi}(T) = \left\langle \frac{\pi}{Mk}\sum_{L=0}^{\infty}(2L+1)2\sin^2\eta_{fi,L}(k)\right\rangle_T \tag{4}$$

and

$$\beta_{fi}(T) = -\left\langle \frac{\pi}{Mk}\sum_{L=0}^{\infty}(2L+1)\sin 2\eta_{fi,L}(k)\right\rangle_T, \tag{5}$$

respectively, where $k = Mv$ is the wave-number of relative motion, v is the impact velocity and M is the reduced mass of the collision system. Both α and β and expressed in terms of elastic scattering phase shifts $\eta_{fi,L}(k) = \delta_{iL}(k) - \delta_{fL}(k)$ and $\langle F\rangle_T$ is a thermal average

$$\langle F\rangle_T = 4\pi\left(\frac{M}{2k_BT}\right)^{3/2}\int dv v^2 e^{-Mv^2/2k_BT}F(v) \tag{6}$$

over the Maxwell velocity distribution at temperature T for the pionic helium-helium system and k_B is the Boltzmann constant. The partial wave phases

$\delta_L(k) = \delta_L(k, R \to \infty)$ are obtained from the asymptotic solution of the variable phase equation [14]

$$\frac{d}{dR}\delta_{nlL}(k,R) = -\frac{2MV_{nl}(R)}{k}\Big[\cos\delta_{nlL}(k,R) j_L(kR) - \sin\delta_{nlL}(k,R) n_L(kR)\Big]^2, \quad (7)$$

subject to the boundary condition $\delta_{nlL}(k,0) = 0$, and $\{j_L(z), n_L(z)\}$ are the Riccati-Bessel functions.

3 Numerical results and discussion

Table 1 and Table 2 present values for the scattering phase shifts $\eta_{fi,L}(k)$ for the "favored" transition $(17,16) \to (16,15)$ and for the "unfavored" one $(16,15) \to (16,14)$, respectively. For the unfavored transition in Table 1, scattering phases are appreciably less than 1 radian over the whole range of wave numbers. In this regime of weak collisions, the phase shifts are added linearly and contribute to the line shift Δ, but have little effect on the broadening Γ. Since all phases are negative, the transition frequency undergoes a blue shift. For $k < 0.5$, the scattering of s, p and d-waves gives dominant contribution to the dipole transition lineshape, contributions of partial waves with $L \geq 3$ are suppressed due to large centrifugal barrier. Larger number of partial waves is required to converge Δ and Γ for $k > 0.5$. The elastic scattering phase shifts associated with the favored transition are shown in Table 2, scattering phases are positive and have appreciable values resulting in red-shift and substantial broadening of the transition line. The principal contribution to the shift and broadening is due s- and p-wave scattering, the d-wave scattering is less pronounced. Since the s-wave phase shift $\eta_0 \to \pi$ near $k \to 0$, the scattering potential in the initial state $V_{17,16}(R)$ supports a single bound state. Because the s-wave scattering is dominant towards threshold, this bound state affects dramatically the transition

Table 1. Phase analysis of the collisional shift and broadening of dipole transition line shape $(n,l) = (16,15) \to (n'l') = (16,14)$ in pionic helium interacting with gaseous helium at temperature $T = 6$ K. Partial phase shifts $\eta_{fi}(k)$, $L = 0, \ldots, 8$ in radians, k is the wave-number of relative motion

	L								
k, a.u.	0	1	2	3	4	5	6	7	8
	$\eta_{fi}(k)$, rad								
0.127	-0.126	-0.047	-0.001	0.000	0.000	0.000	-0.000	0.000	0.000
0.310	-0.063	-0.067	-0.041	-0.007	-0.001	0.000	0.000	0.000	0.000
0.538	-0.047	-0.048	-0.047	-0.036	-0.014	-0.004	-0.001	0.000	0.000
0.805	-0.044	-0.043	-0.041	-0.038	-0.032	-0.019	-0.009	-0.004	-0.002
1.131	-0.046	-0.045	-0.043	-0.040	-0.035	-0.030	-0.022	-0.013	-0.007

Table 2. Phase analysis of the collisional shift and broadening of dipole transition line shape $(n,l) = (17,16) \to (n'l') = (16,15)$ in pionic helium interacting with gaseous helium at temperature $T = 6$ K. Partial phase shifts $\eta_{fi}(k)$, $L = 0,\ldots,8$ in radians, k is the wave-number of relative motion

	L								
k, a.u.	0	1	2	3	4	5	6	7	8
	$\eta_{fi}(k)$, rad								
0.127	0.382	0.115	0.000	0.000	0.000	0.000	0.000	0.000	0.000
0.310	0.243	0.226	0.083	0.002	-0.002	0.000	0.000	0.000	0.000
0.538	0.230	0.219	0.183	0.087	0.009	0.000	0.000	0.000	0.000
0.805	0.248	0.238	0.217	0.177	0.103	0.025	0.006	-0.001	0.000
1.131	0.280	0.273	0.257	0.231	0.192	0.133	0.061	0.013	0.000

line shape at very low speeds with $k < 0.1$ as the center frequency undergoes a blue shift when $\eta_0 > \pi/2$. However the thermally-averaged shift and width are weakly affected by the low-velocity tail in the Maxwell distribution.

Table 3 presents numerical results on the temperature dependence of the slopes of the collisional shift and broadening, $\beta_{fi}(T)$ and $\alpha_{fi}(T)$, of the two transition lines of known experimental interest [15]. The temperature dependence of the line profile is relatively weak in gaseous helium. At low perturber density $N = 10^{21}$ cm^{-3}, the resonance frequency of the unfavored transitions $(n,l) = (16,15) \to (16,14)$ and $(16,15) \to (17,14)$ are blue shifted with $\Delta \approx 2.5$ GHz and $\Delta = 18$ GHz, respectively. For the favored transition $(17,16) \to (16,15)$ the line center undergoes a red-shift with $\Delta \approx -8$ GHz. The large collisional broadening of the transition line $(16,15) \to (17,14)$ $\Gamma = 7.7$ GHz would not allow the transition wavelength to be determined to a fractional precision better than 1 ppm. Because the collisional broadening of the transition line $(16,15) \to (16,14)$ is $\Gamma = 0.1$ GHz, this unfavored transition is suitable for spectroscopic measurements in pionic helium.

To further analyze the effect of the interaction energy $V(r,R,\theta)$ in the $\mathrm{He}^+\pi^-$-He collision system, in Figures 1(a-b) we plot the effective state dependent potentials for the transitions $(17,16) \to (16,15)$ and $(16,15) \to (16,14)$, respectively, together with the potential energy differences $\Delta V = V_i - V_f$. A general

Table 3. Slope of the density shift and broadening $\beta(\alpha)$ for selected transitions in pionic helium and temperatures in the range $4-12$ K, in units of 10^{-21} GHz cm^3

	T (K)				
Transition	4	6	8	10	12
$(16,15) \to (16,14)$	2.97(0.16)	2.93(0.14)	2.92(0.13)	2.93(0.12)	2.94(0.11)
$(16,15) \to (17,14)$	17.56(7.73)	17.97(7.19)	17.95(6.98)	17.94(6.68)	18.07(6.42)
$(17,16) \to (16,15)$	-7.45(1.55)	-7.55(1.41)	-7.78(1.43)	-8.00(1.47)	-8.23(1.52)

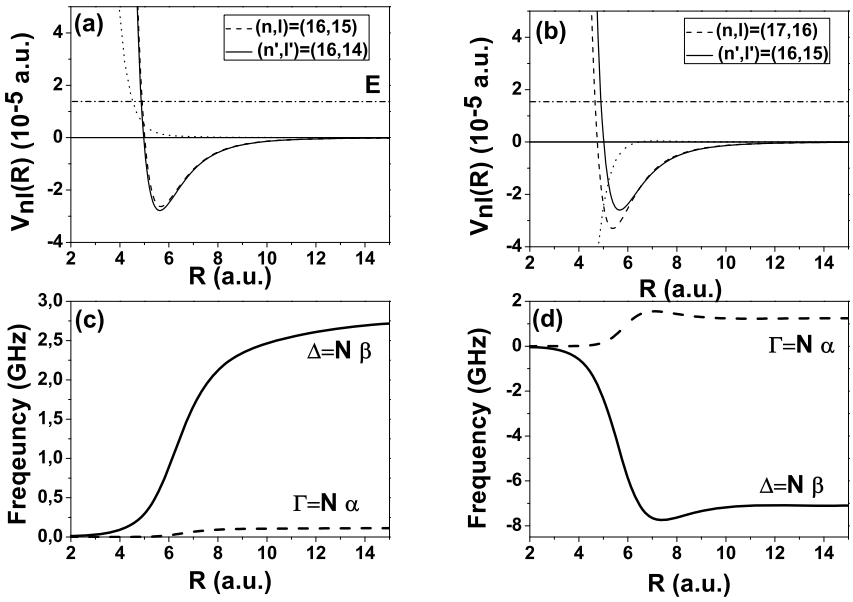

Figure 1. (a) and (b) Potential energy curves $V_{nl}(R)$ for the elastic scattering of pionic helium atoms by an ordinary helium atom prior to (dashed line) and after (solid line) the absorption of a photon in laser-stimulated dipole transitions $(16,15) \rightarrow (16,14)$ and $(17,16) \rightarrow (16,15)$, respectively. The potential energy difference $\Delta V = V_{nl} - V_{n'l'}$ is given by a dotted line, and the kinetic energy of relative motion is indicated by the dashed-dotted line. (c) and (d) Variable line shift and broadening (in GHz) corresponding to the potential energy curves in (a) and (b).

property of the state-dependent potentials is that they are short-ranged, exhibit a hard repulsive part for $R < 5$ a.u. and display a potential minimum located near $R \approx 6$ a.u.. In the variable phase-function approach, Figures 1(c-d) represent the corresponding position-dependent line shift $\Delta(R) = N\beta(R)$ and broadening $\Gamma(R) = N\alpha(R)$ functions at thermal collision energy with $T = 6$ K. The variable line-shift $\Delta(R)$ and width $\Gamma(R)$ functions are defined through Eq.(4) and Eq.(5) in terms of the local phase shift $\eta_{fi}(k,R) = \delta_i(k,R) - \delta_f(k,R)$. For the unfavored transition, the phase functions involve primary weak distant collisions with $R > 5$ a.u. The broadening function saturates rapidly until $R = 8$ a.u., while the shift function saturates much more slowly due to the contributions of higher partial waves with $L > 2$ (large impact parameter). The contribution of close-range binary encounters with $L = 0, 1$ is weakened, because of smaller statistical weight $(2L + 1)$. In contrast, the line shape of the favored transition is primary determined by stronger collisions involving s- and p-wave scattering. Essential part of the line shift (and width) comes from the classically forbidden region for the relative motion with $4 < R \leq 5$ a.u. the shift function rises

steeply in the classically allowed part of the scattering potentials $R > 5$ a.u., attains maximum near $R \approx 7$ a.u., then slightly falls off and saturates in the asymptotic region with $R > 9$ a.u. Thus for this favored transition, the principal part of the line shift and width at thermal collision energies is due to short-range binary encounters, in this case the effect of the long-range van-der-Waals tail $V(R) \sim C_6/R^6$ can be treated as a weak perturbation.

4 Conclusion

We calculated the density shift and broadening of selected dipole transition lines in pionic helium in gaseous helium. At thermal collision energies, we find blueshift of the line center of the unfavored transitions $(n, l) = (16, 15) \rightarrow (16, 14)$ and $(n, l) = (16, 15) \rightarrow (17, 14)$, the transition frequency is red-shifted for a favored transition $(17, 16) \rightarrow (16, 15)$. The negligible collisional broadening ($\Gamma = 0.1$ GHz) of the resonance transition $(n, l) = (16, 15) \rightarrow (16, 14)$ makes it suitable candidate for precision spectroscopy of pionic helium atoms. The theoretical result may be helpful in the extrapolation of the transition wavelengths in pionic helium to zero density of the perturbing helium gas.

References

[1] B. Jeckelmann, T. Nakada, W. Beer, G. de Chambrier, O. Elsenhans, K.L. Giovanetti, P.F.A. Goudsmit, H.J. Leisi, A. Rüstechi, O. Piller, W. Schwitz, *Phys. Rev. Lett*. **56** (1986) 1444.

[2] B. Jeckelmann, W. Beer, G. de Chambrier, O. Elsenhans, K.L. Giovanetti, P.F.A. Goudsmit, H.J. Leisi, T. Nakada, O. Piller, A. Rüstechi, W. Schiwtz, *Nucl. Phys. A* **457** (1986) 709.

[3] M. Hori *et al.*, *Hyperfine Interact.* **233** (2015) 83.

[4] J.G. Fetkovich and E. . Pewitt, *Phys. Rev. Lett*. **11** (1963) 290.

[5] G.T. Condo, *Phys. Lett*. **9** (1964) 65.

[6] S.N. Nakamura, M. Iwasaki, H. Outa, R.S. Hayano, Y. Watanbe, T. Nagae, T. Yamazaki, H. Tada, T. Numao, Y. Kuno and R. Kadono, *Phys. Rev. A* **45** (1992) 6202.

[7] M. Hori A. Söter, V.I. Korobov, *Phys. Rev. A* **89** (2014) 042515.

[8] E. Lindholm, *Arkiv Mat. Astron. Fysik* **28B** (1941) 3.

[9] M. Baranger, *Phys. Rev*. **111** (1958) 481.

[10] N. Allard, J. Kielkopf, *Rev. Mod. Phys*. **54** (1992) 1103.

[11] P.W. Anderson, *Phys. Rev.* **86** (1952) 809.

[12] B. Jeziorski and K. Szalewicz, in *Encyclopedia of Computational Chemistry*, edited by P. von Ragué Schleyer, N.L. Allinger, T. Clark, J. Gasteiger, P.A. Kollman, H.F. Schaefer III, and P.R. Schreiner (Wiley, Chichester, UK, 1998), Vol. 2, p. 1376; B. Jeziorski, K. Szalewicz, and G. Chalasinski, *Int. J. Quantum Chem*. **14** (1978) 271.

[13] D. Bakalov, *Hyperfine Interact*. **233** (2015) 127.

[14] F. Calogero, *Variable phase approach to potential scattering*, (Academic Press, 1967).

[15] M. Hori, Private communication.